31st Annual International Conference of the IEEE EMBS
Minneapolis, Minnesota, USA, September 2-6, 2009

Improved Diagnostics through Quantitative Ultrasound Imaging

David P. Hruska, Jose Sanchez and Michael L. Oelze, *Member, IEEE*

***Abstract*—Conventional B-mode imaging in ultrasound consists of displaying the log-compressed envelope of the backscattered signal. While clinical ultrasonic B-mode images have good spatial resolution, i.e., better than a millimeter, the contrast resolution of ultrasonic B-mode images is typically low. However, additional information is contained in the ultrasonic backscattered signal, which can be used to create images related to tissue microstructure. Because diagnosis of disease is typically based on histological examination of tissue microstructure, the ability to quantify and describe tissue microstructure through ultrasound may result in improved diagnostic capabilities of ultrasound. Tissue-mimicking phantoms and animal models of breast cancer were used to assess the ability of novel ultrasonic imaging techniques to quantify microstructure. Four parameters were extracted from the ultrasonic backscattered signal and related to the microstructure. The effective scatterer diameter (ESD) and the effective acoustic concentration (EAC) parameters were based on modeling the frequency dependence of the backscatter. The k parameter (which quantifies the periodicity of scatterer locations) and the μ parameter (which estimates the number of scatterers per resolution cell) were based on modeling the statistics of the backscattered envelope. Images constructed with these parameters resulted in an increase in contrast between diseased tissue and normal tissues but at the expense of spatial resolution. Specifically, in simulation, quantitative ultrasound (QUS) increased the contrast-to-noise ratio (CNR) between targets and background by more than 10 times in some cases. Statistically significant differences were observed between three kinds of tumors using the ESD, EAC, and k parameters. QUS imaging was also improved with the addition of coded excitation. A novel coded excitation technique was used that improved the variance of estimates over conventional pulsing methods, e.g, the variance of ESD estimates were reduced by a factor of up to 10.**

I. Introduction

Diagnostic medical ultrasound is a fast, safe, non-invasive, and inexpensive imaging modality [1], [2]. Because of these factors, ultrasonic imaging is an attractive approach for the detection and monitoring of disease. In fact, the use of ultrasound to observe morphological structures associated with disease dates back over 55 years [3].

An even more robust diagnostic capability for ultrasonic imaging is possible if tissue microstructure could be imaged because diagnosis of disease is often based on microscopic evaluation of tissues. However, the histopathologic features used to make diagnoses may be as small as 5 μm [1]. Assuming a propagation speed for ultrasound of 1540 m/s, the frequency required to achieve a 5 μm wavelength (the resolution of the imaging system) is over 300 MHz. Along with the present technical difficulties associated with the production of high frequency ultrasound, the attenuation of high-frequency ultrasound in tissues limit the penetration depth used in practice. Typical clinical ultrasound systems employ frequencies in the range of 1 to 15 MHz [4], [5]. A focused (f/2.4) 10 MHz linear array transducer typical of current clinical ultrasound systems has a penetration depth of roughly 5 cm assuming a linear attenuation coefficient of 0.5 dB MHz^{-1} cm^{-1}. Considering only diffraction effects, the ideal axial resolution is 0.33 mm, and the ideal lateral resolution is 0.26 mm [6]. Therefore, the direct imaging of tissue microstructure on the scale of 10s of micrometers or less is not feasible, and alternative approaches have to be used instead. Adding to the difficulties of making diagnoses is the low contrast associated with ultrasonic imaging often observed between diseased and normal tissue and the qualitative nature of ultrasonic B-mode imaging.

Quantitative ultrasound (QUS) imaging techniques have been developed that provide information about tissue microstructure on the order of 10s of micrometers. While the QUS imaging techniques do not resolve tissue microstructure, these techniques provide statistical parameters describing the microstructure. Maps of these parameter values can be generated to construct QUS images that can help in identification and classification of tissues.

The paper is organized as follows: Section II briefly describes the methodology used to extract the tissue microstructure parameters. Section III provides results and discussion from simulations and experiments with animal models of cancer. The conclusions regarding the study are provided in Section IV.

II. Methodology

A. Spectral Parameters

Conventional B-mode images were acquired from tumors using transducers that spanned frequency ranges from 5 to 25 MHz. The tumors consisted of eight benign,

Manuscript received April 20, 2009. This work was supported in part by the National Institutes of Health under Grants CA111289, EB006741, and CA 079179.

D. P. Hruska is with the Department of Electrical and Computer Engineering, University of Illinois at Urbana-Champaign, Urbana, IL 61801 USA. (e-mail: dhruska2@illinois.edu)

J. R. Sanchez is with the Department of Electrical and Computer Engineering, University of Illinois at Urbana-Champaign, Urbana, IL 61801 USA. (e-mail: jsanch27@illinois.edu)

M. L. Oelze is with the Department of Electrical and Computer Engineering, University of Illinois at Urbana-Champaign, Urbana, IL 61801 USA. (phone: 217-333-9226; fax: 217-244-0105; e-mail: oelze@illinois.edu).

spontaneously occurring fibroadenomas in rats, 10 mouse mammary carcinomas, and 10 mouse mammary sarcomas. The rodent tumors were animal models of breast cancer in humans [7]. The backscattered power spectra were measured for many regions of interest (ROIs) within the tumors. The ROIs corresponded to five beamwidths laterally and 12 pulse lengths axially (gated with a Hanning window). The measured backscattered power spectrum for an ROI was found by averaging the backscattered power spectra estimated from the gated echo signals corresponding spatially to the ROI. The measured backscattered power spectrum is given by [8]

$$W_{meas}(f) = \frac{1}{N} A(f,L) \sum_{n=1}^{N} \frac{\left| FT\left\{ p_n(t) \right\} \right|^2}{W_{ref}(f)} \qquad (1)$$

where $FT\left\{ p_n(t) \right\}$ represents the Fourier transform of the gated RF signal of the nth scan line, N is the number of gated scan lines contained within a ROI, $A(f, L)$ is a frequency-dependent attenuation-compensation function and $W_{ref}(f)$ is the reference power spectrum [9]. The effects of the equipment on the power spectrum measurement were factored out by dividing by a reference spectrum [10]. The reference power spectrum was obtained by recording RF signals from reflections off a smooth planar surface of known reflectivity normal to the transducer beam axis. The planar reflector was translated from location at the front of the depth of field of the transducer to the back of the depth of field with a distance of 75 μm (the wavelength at 20 MHz) between steps. At each point the RF signal reflected from the smooth planar surface was recorded. The reference power spectrum for an ROI was calculated by averaging the squared magnitude of the Fourier transform of each reflected RF signal corresponding to the axial location of the ROI [11]. The measured backscattered power spectrum was compensated for attenuation losses according to the frequency-dependent attenuation-compensation function, $A(f, L)$, derived for an echo signal that was gated with a Hanning window [9].

Estimates of the effective scatterer diameter (ESD) and the effective acoustic concentration (EAC) were obtained by comparing the measured power spectrum from eq. (1) to a theoretical power spectrum. The ESD describes the size of the microstructure giving rise to the scattered signal and the EAC describes the number density of scatterers times the square of the impedance difference between the scatterers and background. ESD and EAC estimates were obtained for each ROI.

B. Envelope Statistics

The homodyned K distribution [12] was used to model the amplitude distribution of backscattered ultrasound from the tumors. The model yields two independent parameters related to tissue microstructure: the effective scatterer number density, i.e., the effective number of scatterers per resolution cell (μ parameter) and a parameter related to the periodicity of scatterer locations (k parameter).

The analysis of each tumor was divided into many overlapping ROIs as in the spectral parameter estimation. Extending previous work [13], envelope statistics parameter estimation was performed by first calculating the SNR, skewness, and kurtosis of fractional-order moments of the envelope samples in each ROI. The use of fractional-order moments was motivated by previous work [14], [15] which found that parameter estimates based on fractional-order moments were more robust than parameter estimates based on higher-order moments for the simpler, but related, K distribution. Parameter estimates were deduced by performing a minimum mean-squared error fit between the estimates of SNR, skewness, and kurtosis and theoretical values predicted by the homodyned K distribution. As in [13], the use of SNR, skewness, and kurtosis allowed an efficient estimation algorithm to be implemented.

C. Coded Excitation

A method for improving the contrast and axial resolution of QUS parametric images by using the resolution enhancement compression (REC) technique was incorporated in the study [16]. REC is a coded excitation and pulse compression technique that improves the axial resolution and enhances the -6-dB bandwidth of an ultrasonic imaging system. The variance of spectral estimates can be reduced with increased bandwidth in the imaging system [17]. The objective of using the REC technique was to improve the variance of ESD estimates because of the increased SNR and increased bandwidth provided by REC. Simulations were conducted with a single-element transducer (f/4) having a nominal center frequency of 10 MHz and a -6-dB bandwidth of 80%. Using REC, the -6-dB bandwidth was enhanced to 155%. Images and estimates of scatterer properties using the REC technique were compared with images and estimates using conventional pulsing (CP) techniques. In simulations, a software phantom with cylindrical lesions was evaluated. The software phantom contained cylindrical lesions filled with spherical Gaussian scatterers of 30, 60 and 90 μm in diameter in a background filled with spherical Gaussian scatterers of 50 μm in diameter. Improvements in REC-QUS over conventional QUS were quantified through estimate variance and contrast-to-noise ratio (CNR) of QUS parameter images. The CNR of QUS images were also compared to the CNR of conventional ultrasonic B-mode images.

D. Parametric Image Formation

Parametric images were constructed by superimposing color-coded pixels on a conventional gray-scale B-mode image of the tumors or phantoms. The size and location of the color-coded pixels corresponded to ROIs from which estimates related to microstructures were obtained. For the spectral estimates, a sliding Hanning window was used axially to range gate the signals corresponding to the ROIs with an overlap of 75%. For the estimates from the envelope statistics a rectangular window was used as the range gate function. Laterally, each ROI overlapped the next ROI by 75%. Therefore, each pixel represents at maximum

the average from 16 ROIs. The color of the pixels corresponded to the value of the parameter estimated for each ROI. The resulting color-coded pixels represented maps of the underlying tissue properties as described by the estimates. Four registered parameter images could be generated for each sample examined.

III. Results

Mean estimates of the ESD, EAC, μ parameter and k parameter along with the standard deviation of the estimates are listed in Table I. These estimates represent the average estimate for a particular kind of tumor. Estimates of the p-values between pairs of tumors were obtained through ANOVA and these results are also displayed in Table I. Statistically significant differences were observed between estimates of ESD, EAC, and k for all of the three kinds of tumors examined. Statistically significant differences were observed between the Estimates of the μ parameter did not result in the observation of statistically significant differences between the any pairs of tumors examined.

Parameter images using the estimates from spectral and envelope statistics for each of the kinds of tumors are shown in Fig. 1. The most prominent differences in the images can be observed with parametric images constructed using the ESD and EAC parameters. However, use of multiple parameters resulted in improved classification of the tumors over using just a single parameter for classification. The improved classification using a multiple parameter approach can be illustrated through the feature analysis plot of Fig. 2. A clear separation is observed when plotting the parameter values estimated for each tumor in the feature analysis plot. Simple lines can be drawn between the three kinds of tumors suggesting the ability to clearly differentiate (i.e., diagnose) between the three kinds of tumors examined.

Table I. Average estimates of the ESD, EAC, μ parameter and *k* parameter from three kinds of tumors.

	Power spectrum parameters		Envelope statistics parameters	
	ESD (μm)	EAC (dB)	*k*	*μ*
Carcinomas	42.0 ± 4	16.4 ± 17	0.60 ± 0.07	3.95 ± 3.6
Sarcomas	32.1 ± 4	36.4 ± 12	0.45 ± 0.03	2.28 ± 1.7
Fibroadenomas	107 ± 13	-15.2 ± 5	0.54 ± 0.04	3.31 ± 1.5
	p < 0.05	p < 0.05	p < 0.05	p > 0.5

The use of coded excitation, i.e., the REC technique, resulted in improved depth of penetration for making estimates and a decrease in the variance of ESD estimates [18]. Figure 3 shows images of the software phantom used to demonstrate the improvements introduced by using the REC technique with QUS imaging. Table II lists the CNR and the estimate variance values for the B-mode images and the QUS images.

Improvements in the conventional B-mode images can be observed when using the REC technique over CP techniques. The spatial resolution of the B-mode images was improved using REC technique, which can be identified by the smaller speckle size in the REC B-mode images and the improved definition of the lesion margins. In addition, a small improvement in the CNR was observed for the REC technique compared to the CP technique.

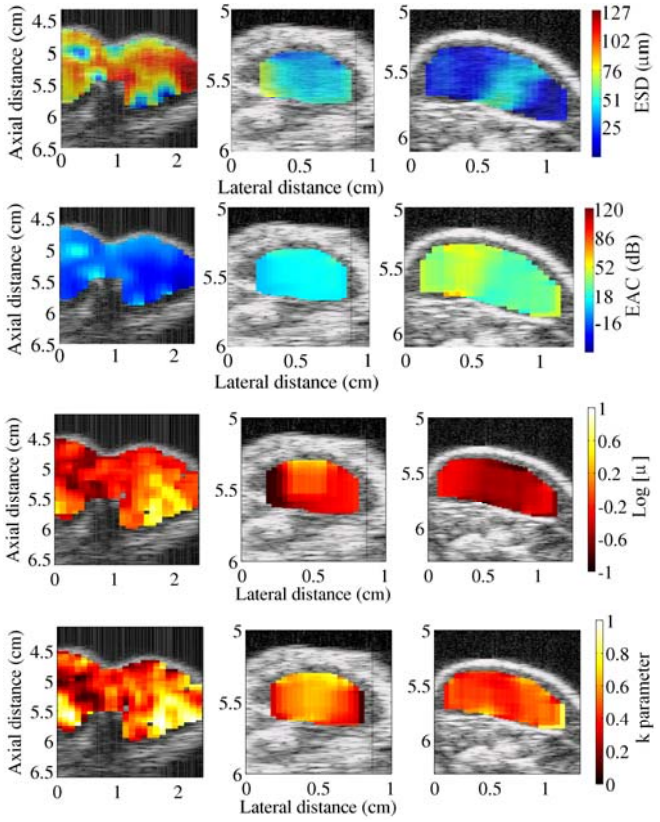

Figure 1. Parametric images of three kinds of tumors (left) fibroadenomas, (middle) carcinomas, and (right) sarcomas using (top two panels) spectral estimates and (bottom two panels) estimates from the envelope statistics.

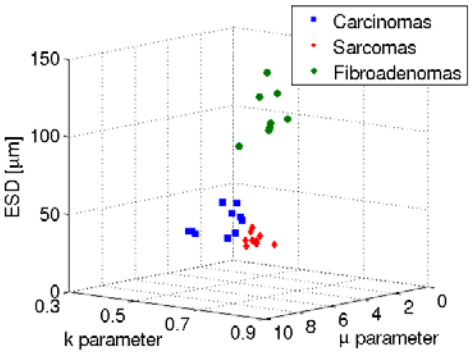

Figure 2. Feature analysis plot of the ESD versus the k parameter versus the μ parameter.

The variance of QUS estimates were also observed to improve with the use of REC over CP. Because of the increased bandwidth from the REC technique, the variance of QUS estimates decreased resulting in smoother images of the cylindrical lesions in the QUS images. In addition, the CNR, which describes the contrast resolution for QUS imaging, was observed to increase when using the REC technique for creating parametric images of ESD.

Finally, the contrast between the cylindrical lesions was increased using QUS imaging over conventional B-mode imaging. Specifically, the CNR of the QUS images increased in some cases by an order of magnitude over the conventional B-mode images. These improvements could result in improved diagnostic performance over conventional methods.

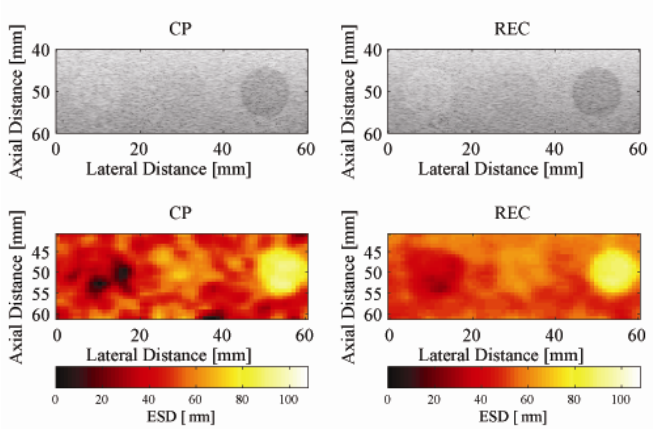

Figure 3. (top panels) B-mode images of software phantom with three cylindrical targets using CP and REC, and (bottom panels) parameter images using the ESD of the software phantom constructed with CP and REC techniques.

Table II. Estimates of CNR and variance of ESD estimates for the B-mode images and the QUS images using CP and REC techniques.

Diameter [μm]	CNR				Variance of ESD	
	CP		REC		CP	REC
	B-mode	QUS	B-mode	QUS		
30	0.28	2.28	0.33	3.31	73.3	16.4
60	0.17	1.45	0.19	3.66	22.9	2.29
90	0.83	6.67	0.85	16.8	2.93	1.11

IV. Conclusion

QUS imaging was observed to significantly improve the ability to classify disease by increasing the contrast between diseased and healthy tissue and by providing estimates of the tissue microstructure. A novel coded excitation was used to decrease the variance of ESD estimates thereby improving the CNR of QUS imaging. Future work will look at constructing new scattering models based on histological analyses, translating these techniques for clinical application, and examining the use of coded excitation for improving accuracy and precision of other QUS estimates.

Acknowledgment

The authors would like to thank Roberto Lavarello, Steven Kanzler, and William D. O'Brien, Jr. for their assistance in the successful completion of this work.

References

[1] J. M. Mamou, "Ultrasonic characterization of three animal mammary tumors from three-dimensional acoustic tissue models," Ph.D. dissertation, University of Illinois at Urbana-Champaign, Urbana, IL, 2005.
[2] W. N. McDicken, *Diagnostic Ultrasonics: Principles and Use of Instruments*. New York: John Wiley & Sons, Inc., 1976.
[3] J. J. Wild and J. M. Reid, "Application of echo-ranging techniques to the determination of structure of biological tissues," *Science*, 115, 226-230, 1952.
[4] W. Huang, "Enhanced image quality reconstruction in medical ultrasound imaging," Ph.D. dissertation, University of Virginia, Charlottesville, VA, 2008.
[5] A. S. Tunis, "Monitoring structural changes in cells and tissues with high frequency ultrasound signal statistics," M.S. thesis, University of Toronto, Toronto, ON, Canada, 2005.
[6] M. F. Insana, "Ultrasonic imaging," in *Wiley Encyclopedia of Biomedical Engineering*, M. Akay Ed. John Wiley & Sons, Hoboken, NJ, 2006, pp. 3640-3648.
[7] M. L. Oelze, J. F. Zachary, and W. D. O'Brien, Jr., "Differentiation and characterization of mammary fibroadenomas and 4T1 Carcinomas using ultrasound parametric imaging," *IEEE Trans Med Imag.* 23, 764-771, 2004.
[8] F. L. Lizzi, M. Astor, T. Liu, C. Deng, D. J. Coleman, and R. H. Silverman, "Ultrasonic spectrum analysis for tissue assays and therapy evaluation," *Int J Imaging Syst Technol* 8, 3-10, 1997.
[9] M. L. Oelze, W. D. O'Brien, Jr., "Frequency-dependent attenuation-compensation functions for ultrasonic signals backscattered from random media," *J Acous Soc Am* 111,2308-2319, 2002.
[10] F. L. Lizzi, M. Greenebaum, E. J. Feleppa, M. Elbaum, D. J. Coleman, "Theoretical framework for spectrum analysis in ultrasonic tissue characterization," *J Acoust Soc Am* 73, 1366-1373, 1983.
[11] M. L. Oelze and W. D. O'Brien, Jr., "Application of three scattering models to the characterization of solid tumors in mice," *Ultrasonic Imaging*, 28, 83-96, 2006.
[12] V. Dutt and J. F. Greenleaf, "Ultrasound echo envelope analysis using a homodyned K distribution signal model," *Ultrasonic Imaging*, vol. 16, pp. 265 287, 1994.
[13] M. Martin-Fernandez, R. Cardenes, and C. Alberola-Lopez, "Parameter estimation of the homodyned K distribution based on signal to noise ratio," *Proceedings of the IEEE Ultrasonics Symposium*, 158-161, 2007.
[14] V. Dutt and J. F. Greenleaf, "Speckle analysis using signal to noise ratios based on fractional order moments," *Ultrasonic Imaging*, 17, 251-268, 1995.
[15] F. Ossant, F. Patat, M. Lebertre, M.-L. Teriierooiterai, and L. Pourcelot, "Effective density estimators based on the K distribution: interest of low and fractional order moments," *Ultrasonic Imaging*, 20, 243-259, 1998.
[16] M. L. Oelze, "Bandwidth and resolution enhancement through pulse compression," *IEEE Transactions on Ultrasonics, Ferroelectrics, and Frequency Control,* 54, 768-781, 2007.
[17] P. Chaturvedi and M. F. Insana, ''Error bounds on ultrasonic scatterer size estimates,'' *J Acoust Soc Am* 100, 392–399, 1996.
[18] J. R. Sanchez, D. Pocci, and M. L. Oelze, "A novel coded excitation scheme to improve spatial and contrast resolution of quantitative ultrasound imaging," *IEEE Trans Ultrason, Ferroelect, Freq Contr,* (accepted).